# An approach to provide maps of the N2O emission risks by soils at the regional scale: A case-study at the Haut-Loir watershed, France

Catherine Pasquier, Hocine Bourennane, Isabelle Cousin, Ghislain Girot, Agnès Grossel, Catherine Hénault

**Title**:

An approach to provide maps of the $N_2O$ emission risks by soils at the regional scale: a case-study at the Haut-Loir watershed, France

**Authors:**

Pasquier Catherine[1], Bourennane Hocine[1], Cousin Isabelle[1], Ghislain Girot[1], Grossel Agnes [1*], Hénault Catherine [2]

[1]INRAE, Info&Sols, F-45075, Orléans, France

[2]INRAE, UMR Agroecologie, F-21078, Dijon, France

***: Corresponding author:**

agnes.grossel@inrae.fr

INRAE, Info&Sols, 2163 avenue de la Pomme de Pin, 45075 Orléans

Tel: France +33 2 38 41 80 48

**Highlights:**

A methodology is developed to map $N_2O$ emission risk based on soil properties.

The hazard and the vulnerability allow inferring the risk of $N_2O$ emissions

This methodology is relevant for all types of soil dedicated to agriculture

Areas where $N_2O$ emissions mitigation actions are possible have been identified.

**Abstract:**

Nitrous oxide ($N_2O$) is often emitted by soils after nitrogen fertilization when the reduction of nitrate into $N_2$ is incomplete and the soil is in hydromorphic condition. To take action to reduce $N_2O$ emissions, it is necessary to identify and locate areas that present a risk of $N_2O$ emissions. In this study, an approach to map $N_2O$ emission risk by soils was therefore developed based on soil properties. The risk of $N_2O$ emission was assessed through two components linked to static properties, independent on climate and agricultural practices; the Vulnerability: the ability of the soil to reduce $N_2O$ and the Hazard: the probability of soil water-logging. This approach was tested in the Haut-Loir watershed (3600 km²), a highly cropped area in the French Center Region. Vulnerability and hazard were estimated using French soil databases. The databases contain the drainage class information which allowed inferring the hazard. They also have measurements of pH, CEC and clay content which

allowed estimating vulnerability through a pedotransfer function. In this watershed, contrasting risks were highlighted between different soil types and agricultural regions. High risk soils (~2% of the studied area) were generally found in valleys and were not under crop because of their hydromorphy and acidity. However, attention should be given to medium risk soils (~32% of the area) which were mainly found in the western region. Oppositely, soils of the eastern region present generally no risk of $N_2O$ emissions. Some former field studies have been reported in the studied watershed: they generally supported this soil risk classification. For medium-risk soils, different actions of mitigation depending on the degree of risk were suggested: liming or adjusting nitrogen input periods. This risk mapping approach could be applied in other cropland regions to help mitigation strategy.

**Keywords***:*

Greenhouse gas; Risk assessment; Vulnerability; Hazard; Exposure; Soil mapping; Multiple soil classes.

**Abbreviations:**

CEC, Cation Exchange Capacity; GHG, Greenhouse Gas; HV, High Vulnerability; HH, High Hazard; HR, High Risk; IPCC, Intergovernmental Panel on Climate Change; Km, Kilometers; LV, Low Vulnerability; LH, Low Hazard; LR, Low Risk; MM, Moderate Vulnerability; MH, Moderate Hazard; MR, Moderate Risk; RP (French), Pedological Referential; RRP, Pedological Regional Referential; STU, Soil Typological Units; SMU, Soil map Units; WRB, World Reference Base for soil resources.

## 1. Introduction

Climate change induced by increased Greenhouse Gases (GHGs) emissions in the atmosphere results in global warming (Masson-Delmotte et al., 2018). Nitrous oxide ($N_2O$) is one of the three main anthropogenic GHGs in the atmosphere. $N_2O$ has about 265 times the warming potential of $CO_2$ (Ciais et al., 2013), but its concentration is more than 1000 times lower than atmospheric $CO_2$ concentration, so its contribution to the greenhouse effect is evaluated for 2020 at about 7% against 66% for $CO_2$ and 16% for $CH_4$ (WMO, 2021). In France, agriculture is the main sector contributing to anthropogenic $N_2O$ emissions and represented about 89% of these emissions in 2019 (Thompson et al., 2019; CITEPA, 2021). Agricultural emissions of $N_2O$ are mainly due to N inputs of mineral and organic fertilizers in soils and a linear relation is assumed between N inputs and $N_2O$ emissions (1% of N input, IPCC Tier-1, Hergoualc'h et al., 2019). In France, since 1990, $N_2O$ emissions have been slightly decreased, from 65.4 to 38.2 Mt $CO_2$e, and emission due to agriculture decreased slowly from 38.2 to 34.5 Mt $CO_2$e (CITEPA, 2021), thanks to the use of more optimized and regulated mineral fertilizers. The "Centre – Val de Loire" region is a region of intensive agriculture where the contribution of agriculture to total $N_2O$ emissions is estimated to be as high as 95% (2.6 Mt $CO_2$e) corresponding to about 14% of all GHGs in $CO_2$e (LIG'AIR inventory V2.4/2020).

Agricultural $N_2O$ emissions exhibit a very large spatial and temporal variability because they are highly dependent on pedoclimatic conditions (e.g., soil concentration of mineral nitrogen, soil moisture, temperature). The $N_2O$ is indeed produced by several microbial processes resulting from the activity of different species of microorganisms (e.g., nitrification, denitrification, nitrifier denitrification…; Butterbach-Bahl et al., 2013) using soil nitrogen as substrate. Denitrification (the reduction of nitrate in several steps, to $N_2O$ and lastly to $N_2$) is considered as one of the most important processes of $N_2O$ production in soils (Dobbie and Smith, 2001). Denitrification occurs in anoxic soils and is therefore favored by soil moisture. Large peaks of $N_2O$ emissions occur in wet soils with high nitrogen (N) levels, usually after input of nitrogen fertilizers (Stehfest and Bouwmann, 2006; Ito et al., 2018). Complete denitrification leads to $N_2$ emission, which is not of environmental concern since $N_2$ is a non-reactive molecule and is not absorbing in the infrared spectrum. The last

82 step of denitrification, the reduction of $N_2O$ in $N_2$, is inhibited in certain soil conditions or in some
83 soils. Therefore, some soils do not present a capacity to reduce $N_2O$ to $N_2$. For example, pH controls
84 the ability of the denitrifying bacteria to express $N_2O$ reductase early and efficiently (Russenes et al.,
85 2016), which probably explains why soil pH influences $N_2O$ emissions when denitrification is the
86 main source of $N_2O$. Previous studies also revealed soil pH as one of the main factors governing
87 regional variability of $N_2O$ emission on a global meta-analysis (Wang et al., 2018). Many studies have
88 been conducted to understand the determinism of $N_2O$ production and reduction, bringing more and
89 more insight into these processes and their controlling factors (Stehfest and Bouwman, 2006; Cui et
90 al., 2021) and the effect of different agricultural practices. This enables to propose some technical
91 solutions to limit $N_2O$ emissions. Avoiding excess soil nitrate, particularly when soils are too wet, can
92 help minimize $N_2O$ emissions from agriculturally managed soils. Other solutions are being studied,
93 like bacterial seeding, draining moist soil, nitrification-inhibiting (e.g. Henault et al., 1998; Rochette,
94 2008; Ruser and Schulz, 2015; Hinton et al., 2015). pH management, i.e. soil liming to raise the pH, is
95 also an important track to reduce $N_2O$ emissions (Henault et al., 2019; Shaaban et al., 2020).

96 However, most studies have been made at field scale, so the representativeness of observations when
97 upscaling (e.g. regional scale) is unclear. $N_2O$ is indeed produced at soil microsite scale and this
98 production is controlled by a complex interaction of factors. Therefore, similar agricultural practices
99 can have different effect on $N_2O$ emission in different soil types (e.g. Rochette et al., 2008). The use of
100 methods to reduce $N_2O$ emissions involve identifying soils which are likely to emit $N_2O$. This is
101 consistent with the findings of Cui et al. (2021), who recently provided a global map of $N_2O$ emission
102 factors (i.e. $N_2O$ emission taking into account nitrogen inputs) based on a data-driven meta-analysis.
103 They outlined that the most policy-relevant question is to identify where emissions can be mitigated
104 more efficiently.

105 It is therefore useful to provide maps of $N_2O$ emissions or emission risk which can indicate where
106 actions have to be taken. Few studies provide spatial assessment of emissions and they generally
107 consider agricultural practices, which can be difficult to obtain. Mapping $N_2O$ emission can be done
108 by applying predictive models: this approach was used by the European Soil Data Centre, who

109 published a map of $N_2O$ emissions from agricultural soil in Europe taking soil properties into account,
110 based on LUCAS soil sampling program and using DayCent model combined with random forest
111 approach (Lugato et al., 2017). The resulting map depends on climatic data inputs and information on
112 managements practices. As $N_2O$ emissions are extremely dependent on climatic conditions, they
113 averaged 5 years of data to smooth the temporal variability. Another method was proposed by Kritee
114 et al. (2018) who mapped risk of large $N_2O$ emissions from rice production taking into account two
115 components: water management regimes and regional N fertilizer rates, but ignoring soil properties. In
116 both cases, the maps are a snapshot of a given situation as climate and management practices are
117 subjected to change. Providing soil $N_2O$ emission risk, based on soil properties, i.e. static or more or
118 less static properties, is a valuable approach for policy-makers. This is consistent with the approach of
119 Cui et al. (2021): they provided a global map of emission factors rather than $N_2O$ emissions. Global
120 information may however have a too coarse resolution for defining mitigation strategies; the best scale
121 would be regional or national, which is also the scale of policy-making. However, Cui et al. (2021)
122 also observed that controlling factors are scale-dependent, so it is very important to further provide
123 regional maps of $N_2O$ emission risk.

124 The objective of this paper was therefore to develop an approach to map at regional scale $N_2O$
125 emission risk based on soil properties. IPCC approach defined risk as the likelihood of harmful
126 alterations due to hazardous physical events interacting with vulnerable conditions (Lavell et al.,
127 2012). They proposed to cross hazard, vulnerability and exposure to fully assess risk, and defined
128 these three notions. Hazard is the potential occurrence of a physical event having adverse effect;
129 vulnerability is the predisposition of an element to be affected due to internal characteristics; and
130 exposure referred to the presence of resources in places that could be affected by the physical events.
131 A similar approach is then developed here for $N_2O$ emission risk. Hazard was considered as soil water
132 excess probability, which leads to conditions favorable to denitrification. Vulnerability was considered
133 to be due to the soil capacity to reduce $N_2O$ in $N_2$, which, as already mentioned, depends on soil
134 properties. Exposure corresponds to soil nitrogen inputs. In this study, vulnerability and hazard were
135 considered simultaneously to provide maps considering only static risk in relation to soil properties.

Soil capacity to reduce $N_2O$ to $N_2$ can be evaluated in the laboratory, using incubated soil samples according to ISO/TS 20131-2 method (Le Gall et al., 2014; Henault et al., 2019). An index, called r-max value, is calculated, which corresponds to the ratio between the amount of $N_2O$ emitted without and with acetylene during incubation because acetylene inhibits the last step of denitrification. The higher is the r-max, the lower is the soil's ability to reduce $N_2O$ to $N_2$. The r-max value can also be estimated by a soil function depending of pH, Cation Exchange Capacity (CEC) and clay content, where pH is the more relevant variable of function (Henault et al., 2019). This function was applied on soil databases. Hazard was assessed by the natural soil hydromorphic class.

Providing $N_2O$ emission risk assessment is especially important in intensive cropland areas receiving large fertilizations. The present approach was thus applied in an intensive cropland region of France. The first step was to map the r-max index using the pedotransfer function and soil variables from a French Soil database. In a second step, the risk approach was tested to assess graduated soil $N_2O$ emissions risk based on the combination of vulnerability and hazard. A former dataset was also used to assess the validity of the soil risk classification. Therefore, this study aims to contribute and improve existing tools and approaches to provide at decision-scale $N_2O$ emission maps from existing soil databases.

## 2. Materials and methods

### 2.1. The study area

The study area is a watershed in the upper valley of Loir River “Haut-Loir”, located in French “Centre Val-de-Loire” region France, that has already been the support of several studies on direct and indirect $N_2O$ emissions (Gu et al., 2013; Grossel et al., 2016; Billen et al., 2018, 2020). It extends over 3600 km² and includes seven agricultural regions: Perche, Faux Perche, Beauce, Beauce Dunoise, Orléanais, Val de Loire and Vallée de Loir (Figure 1). The four main regions (Perche, Faux Perche, Beauce, Beauce Dunoise) represent 90% of the study area and are covered by intensive croplands – usually wheat, barley, maize and rapeseed - that are subjected to high nitrogen inputs.

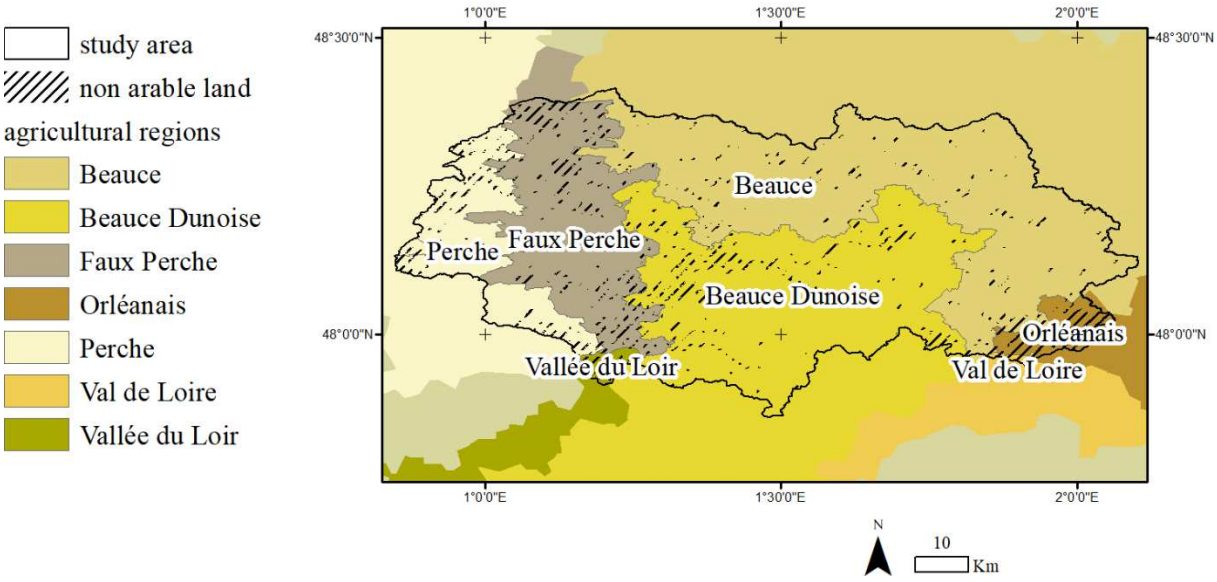


162

163 *Figure 1: Haut-Loir extension, study area*

164 The Loir River consists in a natural limit between the Eastern Beauce/Beauce Dunoise regions and the
165 Western Perche/Faux Perche regions. For the purposes of this regional study, the soil classification
166 was kept in its original repository (RP2008, Baize et al., 2009) described in the French database
167 (Figure 2). The correspondence between the RP2008 and the WRB soil classifications is given in the
168 Appendix A. The match is not easy between the two systems of classification because a soil described
169 in RP2008 can have several matchings in WRB and vice versa. The correspondence depends on many
170 possibilities of qualifying soils that have not been further analysed in this study due to the lack of
171 representativeness at this regional scale.

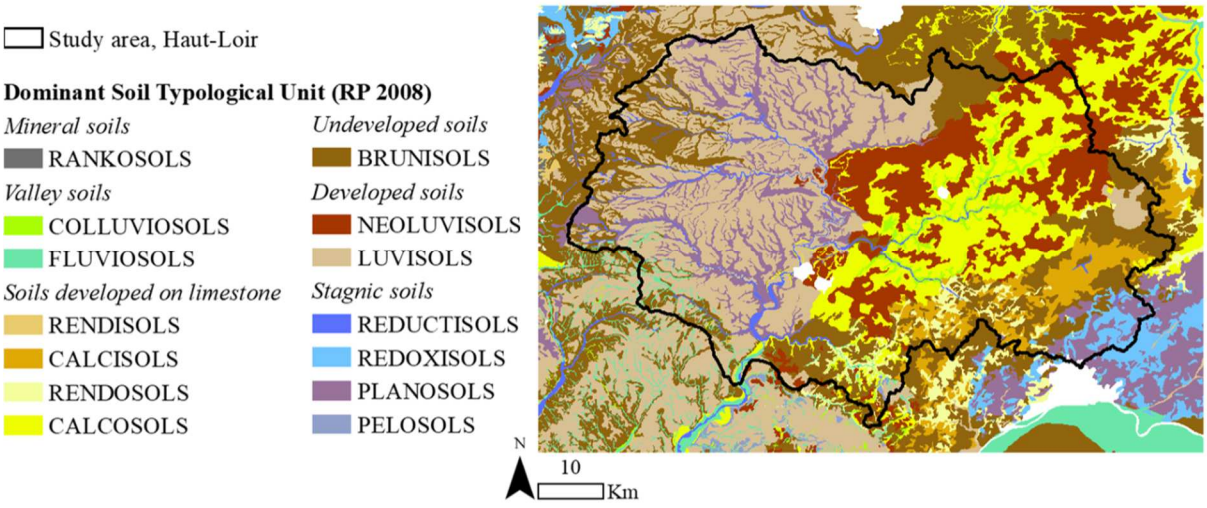


172

*Figure 2: Haut-Loir soils map. Soils are given in regional repository and the correspondence to WRB is given in Appendix A.*

The Western Perche and the Vallée du Loir Region are dominated by hydromorphic LUVISOLS and PLANOSOLS, which are usually drained and limed for agriculture practices (Figure 2). REDUCTISOLS are usually located near streams. In the Beauce/Beauce Dunoise regions, soils are developed on limestone (CALCOSOLS, CALCISOLS and NEOLUVISOLS …): they are more clayey and exhibit a higher pH value. Agricultural soils in these Eastern areas are usually irrigated, which allows maize plant in crop rotation. Orléanais forest region, in the Southwest part of the study area, and the Val-de-Loire Region, are dominated by PLANOSOLS and REDOXISOLS. The white areas in the soils map (Figure 2) correspond to undefined soil (urban areas) where there is no data in DoneSol.

## 2.2. The soil database

We have used a French Soil Geographical database on a scale of 1:250,000: "Référentiels Régionaux Pédologiques", RRPs (Richer-de-Forges et al., 2019). RRPs are regional geographic databases established from field surveys and observations by soil scientists. The data from RRPs are available to users through a national standardized soil information storage system (DoneSol).

Donesol contains a list of Soil Typological Units (**STU**). In RP2008, STU are described by variables specifying the soil type and their properties (soil texture, CEC, pH, soil drainage, etc.). Soil natural drainage is coded from 1 (well-drained soils) to 9 (submerged soils) (Richer-de-Forges et al., 2019; *cf.* Table 1, supplementary material). This indicator provides information on the frequency of excess water in the soil.

At the scale of 1:250,000, it is not possible to delineate the STUs. Therefore, they are grouped into Soil Mapping Units (SMU) to form soil associations and to illustrate the functioning of pedological systems in landscapes. Each SMU corresponds to soil-landscape, i.e. a part of the mapped territory defined by specific pedology, hydrogeology, topology and / or land use. It has a known shape and location and is represented by one or more polygons in a geometrical dataset. Oppositely, STU cannot

be precisely located within SMU. Soil type (STU) can be identified within SMU and is specified as a percentage of SMU area. As a result, RRPs consists of both a geometrical dataset defining SMU and a semantic dataset which links attribute values, including STU and soil variables, to the SMUs. It is the same principle than for Soil Geographical Database of Europe, well-illustrated in the supplementary Figure 1.

For display purpose, the SMU properties are represented with either the dominant STU, or a weighted average of STU areas. Both methods were tested in this study. Database structure is explained in the following link:

(https://esdac.jrc.ec.europa.eu/ESDB_Archive/ESDBv2/esdb/sgdbe/metadata/purity_maps/purity.htm.

### 2.3. R-max index

The r-max index, indicative of the capacity of a soil to reduce $N_2O$ to $N_2$, was calculated for each STU by using soil variables (CEC, pH and clay content) from the DoneSol database according to the following function (Henault et al., 2019 and ISO/TS 20131-2 norm):

$$r\text{-}max = -0.4\ pH + 0.026\ CEC - 0.001\ clay + 3.13\ (r = 0.88)$$

where pH is evaluated on an air-dried sample suspended in water according to the NF ISO 10390 norm, CEC is evaluated on a soil sample extract using a cobalt-hexamine solution (Orsini and Rémi, 1976) according to the NF X 31-130 norm, and clay represents the clay content ($g.g^{-1}$) measured on a soil sample without decarbonation by using the Robinson pipette method according to the NF X 31-107 norm. The r-max values are limited to 1.2.

According to Hénault et al., 2019, soils with an *r-max* > 0.8 have a very low capacity to reduce $N_2O$, soils with *r-max* < 0.4 are able to reduce $N_2O$ and soils with an *r-max* value between 0.4 and 0.8 have an intermediate capacity to reduce $N_2O$. Soil pH explains most of the *r-max* index variability (61%): soils with pH < 6.4 have usually *r-max* > 0.8, and soils with pH > 6.8 have r-max < 0.4, (Hénault et al., 2019).

## 2.4. Definition of $N_2O$ emission risk

Risk of $N_2O$ emission was based on Hazard, Vulnerability and Exposure as suggested in literature (Crichton, 1999; Wolf, 2012; Lavell et al., 2012).

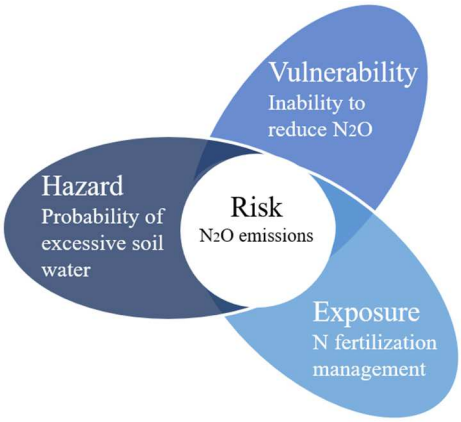


*Figure 3: representation of $N_2O$ emission risk, inspired by core concept of SREX IPCC, 2012*

In our case (Figure 3) Vulnerability corresponds to the soil inability to reduce $N_2O$, natural Hazard is the probability that a situation of excess water occurs, and Exposure corresponds to N fertilization by farmers, leading to an increase in available mineral N into the soil. Hazard can be predicted thanks to precipitations or soil water content measured by in situ sensors. Exposure could be limited by decreasing N inputs. Exposure depends on land use: croplands were considered as the only ones that are subject to nitrogen inputs related to fertilization. For urban area or forest, Exposure is zero.

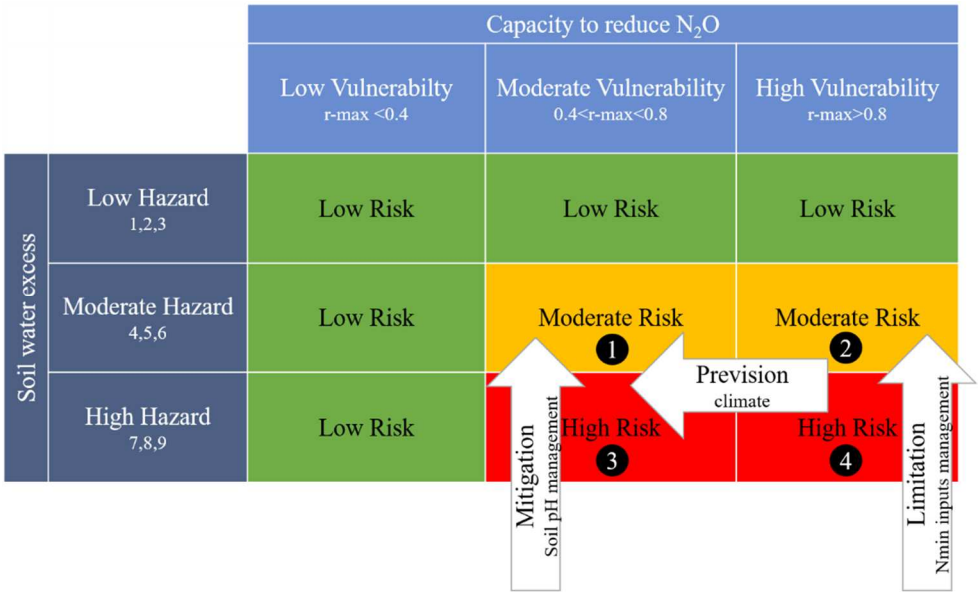

236 *Figure 4: $N_2O$ risk core concept*

237 Three classes of Vulnerability were defined: Low Vulnerability (LV) for *r-max* < 0.4, Moderate
238 Vulnerability (MV) for 0.4<*r-max*<0.8 and High Vulnerability (HV) for *r-max* >0.8. Hazard, i.e.
239 probability of excess water in soils, depends not only on precipitations but also on soil type. Soil
240 drainage class was thus considered to identify areas where excess water may occur. Three classes of
241 Hazards were similarly defined: Low Hazard (LH) for DoneSol soil drain classes 1, 2 and 3, Moderate
242 Hazard (MH) for classes 4, 5 and 6 and High Hazard (HH) for classes 7, 8 and 9. Finally, we defined
243 risk by crossing vulnerability with hazard (Figure 4). However, hazard and vulnerability, as defined,
244 are not controlling $N_2O$ emission risk in the same way. Excess water controls the occurrence of
245 denitrification, i.e. $N_2O$ production in soils. The soil capacity to reduce $N_2O$ in $N_2$ is important only if
246 denitrification and $N_2O$ production can occur, i.e. if there is significant hazard. This is why hazard was
247 considered to have a higher control on risk than vulnerability and the figure 4 is not fully symmetrical.
248 In other words, moderate Risk (MR) corresponds at situations of Moderate Hazard with Moderate or
249 High Vulnerabilities and High Risk (HR) corresponds at situations of High Hazard with Moderate or
250 High Vulnerabilities.

251 Last four risk categories were defined to suggest different mitigation strategies. Vulnerability can be
252 reduced by actions of mitigation. For example, liming soils raises the pH and increases the soil's
253 ability to reduce $N_2O$ (Henault et al., 2019). Categories 1 (moderate risk) and 3 (high risk) correspond
254 to situations of moderate vulnerability that can mostly be mitigated by liming soil when pH < 6.8.
255 Categories 2 and 4 correspond respectively to Moderate Risk and High Risk that can be reduced by
256 liming soil when pH < 6.4 and that further requires special precautions when supplying nitrogen in soil
257 (dose reduction or taking account soil water condition).

258 2.5 Validation data

259 $N_2O$ emission measurements from previous studies (Hénault et al., 2005; Franqueville et al., 2018 and
260 other unpublished studies) were used to validate the present approach. These measurements were
261 carried out over thirteen study sites included in our study area "Haut-Loir".

Thus, $N_2O$ emissions and soil properties are available from direct measurements for one CALCISOLS, six LUVISOLS, two BRUNISOLS and four COLLUVIOSOLS. $N_2O$ measurements were done by static chamber with a frequency varying from once per week to once per month.

All plots were cropped with winter cereals and fertilized with mineral N but at different timing, splitting and amount. Therefore, to compare sites, $N_2O$ emissions were cumulated from the last date before first fertilization to one month after the last fertilization. $N_2O$ peaks generally occur in the weeks following N inputs so this may encompass most of the fertilization effect. The ratio of cumulative emission during post-fertilization period to the N input amount was then calculated for all sites.

Measured r-max values following the protocol of Hénault et al. (2019) were reported when available (measured r-max index). A Calc. r-max index was calculated from soil properties measured on in situ soil samples during the studies and STU r-max index was calculated from the Donesol values of the map soil STU. Drainage classes were inferred from Donesol database. This allowed to assess hazard and vulnerability and to calculate a risk class for each site.

## 3. Results and discussion

### 3.1. Application of the *r-max* function at STU and SMU resolution

#### 3.1.1. *r-max* index computed by STU

DoneSol semantic database was used to infer the *r-max* values for all STU with the values of clay. CEC and pH (85% of STU). This allowed to assess an *r-max* value (Table 1) for each soil type of the study site and thus infer its vulnerability typology (ability to reduce $N_2O$ to $N_2$).

*Table 1: r-max mean value by soil type and associated standard deviation (std). number (nb) of values in each STU and SMU. representativeness in study site (% area) and vulnerability typology.*

| Soil type (RP2008) | nb STU | r-max mean | r-max std | % area | nb SMU | Vulnerability |
|---|---|---|---|---|---|---|

| | | | | | | |
|---|---|---|---|---|---|---|
| CALCOSOLS (CALCO) | 23 | 0.11 | 0.13 | 10 | 25 | LV |
| RENDOSOLS (RENDO) | 11 | 0.14 | 0.14 | 3 | 22 | LV |
| RENDISOLS (RENDI) | 5 | 0.17 | 0.16 | 1 | 10 | LV |
| HISTOSOLS* (HIST) | 1 | 0.25 | | <1 | 1 | LV |
| CALCISOLS (CALCI) | 18 | 0.29 | 0.19 | 6 | 26 | LV |
| FLUVIOSOLS (FLUV) | 19 | 0.42 | 0.26 | <1 | 9 | MV |
| PEYROSOLS (PEYR) | 1 | 0.44 | | <1 | 1 | MV |
| COLLUVIOSOLS (COLL) | 10 | 0.51 | 0.36 | 1 | 7 | MV |
| NEOLUVISOLS (NEO) | 18 | 0.58 | 0.21 | 12 | 20 | MV |
| BRUNISOLS* (BRUN) | 51 | 0.61 | 0.31 | 14 | 45 | MV |
| ARENOSOLS (ARE) | 1 | 0.62 | | <1 | 2 | MV |
| PELOSOLS (PEL) | 3 | 0.63 | 0.10 | <1 | 2 | MV |
| LUVISOLS (LUV) | 50 | 0.64 | 0.22 | 28 | 32 | MV |
| FERSIALSOLS (FER) | 1 | 0.74 | | <1 | 1 | MV |
| PLANOSOLS (PLANO) | 10 | 0.78 | 0.09 | 8 | 15 | MV |
| REDOXISOLS (REDOX) | 6 | 0.80 | 0.37 | 2 | 11 | HV |
| VERTISOLS (VERT) | 1 | 0.86 | | <1 | 1 | HV |
| REDUCTISOLS (REDUCT) | 5 | 0.88 | 0.28 | 1 | 3 | HV |
| ALOCRISOLS (ALO) | 1 | 1.20 | | <1 | 1 | HV |
| PODZOSOLS (PODZ) | 2 | 1.20 | 0.00 | <1 | 2 | HV |

The *r-max* mean values vary from 0.11 (CALCOSOLS, carbonated soil from the surface) to 1.20 (PODZOSOLS, acidic soils). Soil types FERSIALSOLS, HISTOSOLS, ARENOSOLS, VERTISOLS and ALOCRISOLS are less encountered in the study area, thus their *r-max* values must be further confirmed.

The soils with the lowest *r-max* are soils developed on limestone (RENDOSOLS, CALCOSOLS, RENDISOLS and CALCISOLS). These soils have an *r-max* under 0.4, so they are able to reduce $N_2O$. They cover 20% of the Haut-Loir surface and they are mostly to the Eastern of the site (Beauce/Beauce dunoise). For the HISTOSOLS the *r-max* value is 0.25. As HISTOSOLS correspond to peat soils (organic soils) and are often acidic, farmed organic soils appear to emit exceptionally large amounts of $N_2O$ (Kasimir-Klemedtsson et al., 1997). However, in this study the only HISTOSOLS is a eutrophic-peat with pH > 8.

All the other soil types present a mean of *r-max* over 0.4, and some of them are over 0.8 (REDUCTISOLS, REDOXISOLS, VERTISOLS, PODZOSOLS and ALOCRISOLS, for 5% of the study site) and therefore not able to reduce $N_2O$ (HV). Over 60 % of soil surface are classed in MV.

The BRUNISOLS (14 % of the study area) show *r-max* values ranging from 0 to 1.2. In fact, there are two large categories of BRUNISOLS: Eutric BRUNISOLS and Dystric BRUNISOLS Dystric soils have a base saturation (S/CEC: S being the sum of exchangeable cations ($Ca^{2+}$, $Mg^{2+}$, $K^+$ and $Na^+$)) at pH=7 of less than 50 % whereas Eutric soil have a base saturation at pH=7 of 50 % or more (Baize et al., 2009). This soil attribute depends on the CEC and therefore has an influence on the *r-max* value. Dystric BRUNISOLS have an *r-max* mean value upper than 0.8 and Eutric BRUNISOL have a *r-max* value about 0.59, i.e. in the intermediate class.

There is also a large variability in *r-max* values of hydromorphic soils (COLLUVIOSOLS, FLUVIOSOLS, REDOXISOLS and REDUCTISOLS), because these soils could be more or less clayey and more or less acidic.

The value of the *r-max* seems to follow a growth in the direction of soil evolution through the lateralization processes of clay lixiviation and acidification. Low-evolved soils (RENDOSOLS, RENDISOLS, CALCOSOLS and CALCISOLS) have the ability to reduce $N_2O$ to $N_2$, then soils that move towards BRUNISOLS, LUVISOLS, PLANOSOLS lose their ability to reduce $N_2O$ and finally REDUCTISOLS and PODZOSOLS no longer reduce $N_2O$ at all in $N_2$.

This soil evolution is described in soil Atlas of Europe in WRB classification. Cambisols degrade because of vertical water erosion. The continuous leaching moves the calcium carbonate front further downwards, the pH drops to about 6 and clay illuviation starts to become rich Luvisol. However, the leaching will continuously remove the base elements from the soil. This will make the profile so acid that it will be classified as an Alisol. At this stage the soil is so acid that the clay in the illuviated horizon will disintegrate or be redistributed to other parts of the profile and tongues of silt and sand will cut into the clay illuviated horizon. This is referred to as an Albeluvisol. Finally, the leaching will enable an iron pan to develop and the soil turns into a Podzol.

### 3.1.2.r-max aggregation by SMU

SMU *r-max* maps joining data from RRPs and Donesol were carried out with the r-max mean of all STU contained in the SMU weighted by their area (Fig. 5a) and using the soil variables of dominant STU (Fig. 5b). There are many similarities between the two maps. The difference between Eastern and Western regions can be explained by the presence of soils developed on limestone in Beauce/ Beauce Dunoise (CALCOSOLS, RENDOSOLS, RENDISOLS, CALCISOLS) and the more acidic soils in Western regions. Overall Western soils are not able to reduce $N_2O$. The highest *r-max* values are located near the streams and in watershed heads of the Western-Perche/Faux Perche region (REDUCTISOLS and LUVISOLS).

Figures 5c and 5d correspond, respectively, to the standard deviation calculated in the SMU and to the representativeness of the dominant soil in the SMU. The maps show SMU with an *r-max* values > 0.8 in northeast (Beauce) and in southeast (Orléanais). In these areas, the *r-max* standard deviation is > 0.4 (Figure 5d). This suggests a large variation of *r-max* within the SMU due to differences between *r-max* from grouped STU.

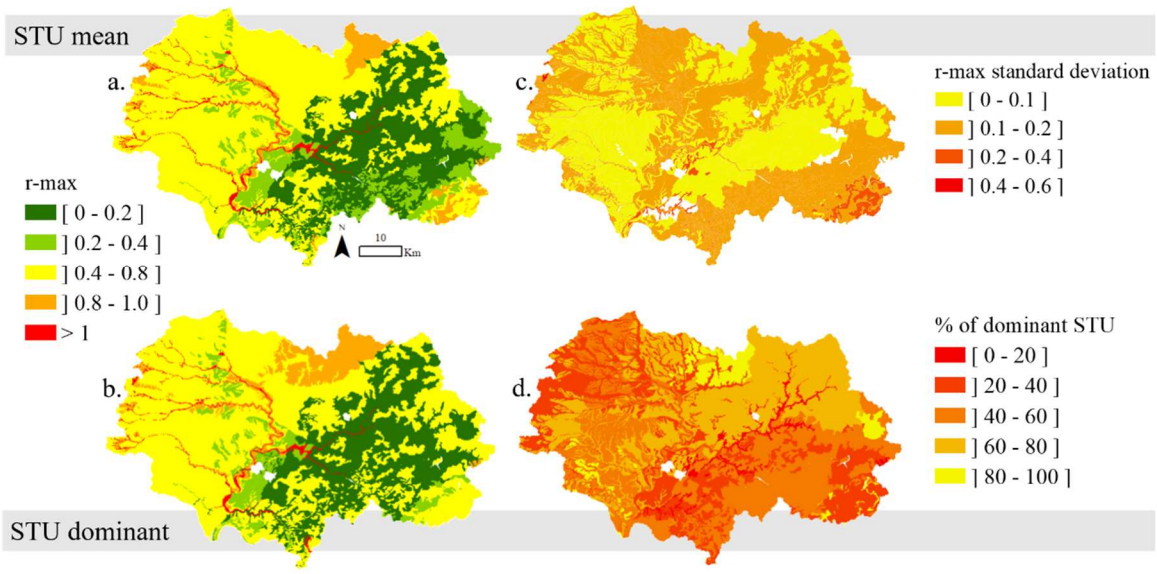


*Figure 5: r-max maps and related standard deviation at study site (Haut-Loir) (respectively with mean and standard-deviation of all STU per SMU: 5a and 5c; and dominant STU values, 5b and 5d). See text for more details.*

SMU aggregation allows to represent spatially the *r-max* at the expense of accuracy. The mean value tends to smooth out extreme values and the dominant STU value is not always representative.

### 3.2. Risk assessment

#### 3.2.1. Vulnerability and Hazard

Figure 6 exhibits the percentage of area of each SMU corresponding to the different Vulnerability and Hazard typologies. This area was estimated based on vulnerability and hazard of the STUs forming the SMU.

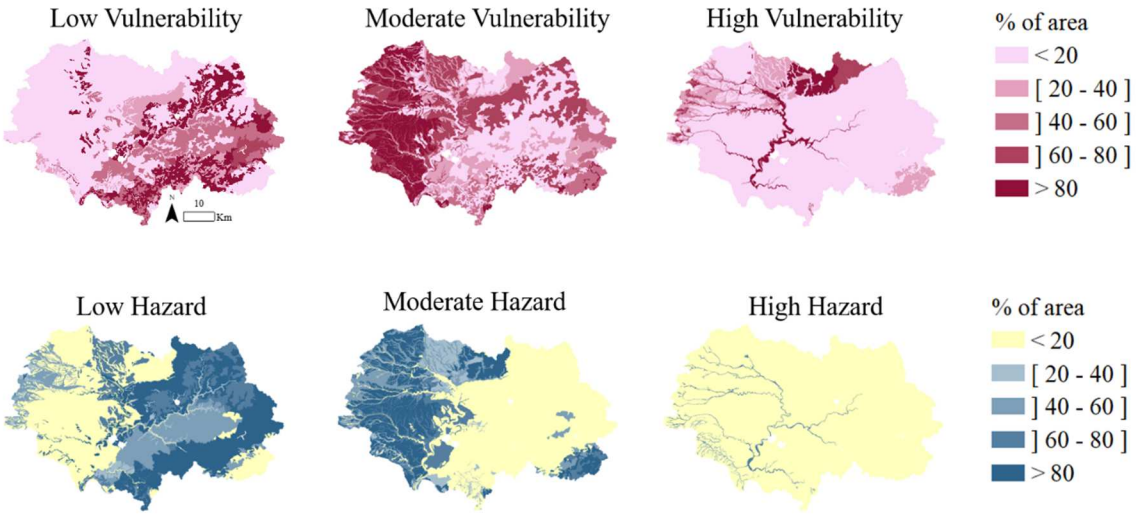


*Figure 6: Vulnerability and Hazard maps estimated at STU scale and expressed in percentage of SMU area*

These maps allow to detect where the most vulnerable soils are located and those subject to the greatest hazards. 15% of soil surface is not classified because of missing values. 29% of soil surface from study site are classified in Low Vulnerability, 44% in Moderate Vulnerability and 12% in High Vulnerability. 49% of soil surface are classified in Low Hazard, 35% in Moderate Hazard and 1% in High Hazard.

Soils with Low Vulnerability and Hazard are mostly located in Eastern Beauce/Beauce Dunoise. Soils with Moderate Vulnerability and Hazard are mostly located in Western Perce/Faux-Perche and Orléanais and soils with High Vulnerability and Hazard are located in valleys.

Hazard and Vulnerability areas are quite similar. Non-vulnerable soils, therefore able to reduce $N_2O$ to $N_2$, seems not to have water excess characteristics. Conversely, vulnerable soils (MV and HV) are generally in a situation of excess soil water (MH and HH). Indeed, excess water in the soil and leaching induce redox processes and increase the soil acidity (Van Breemen and Buurman, 2002), so these that two components are not always independent.

There are still a few special cases: the heads of watersheds on the Western side are classified in HV and LH. There is also an area in North of the Beauce region that is classified in HV (because of low pH value) and which is classified largely in LH.

### 3.2.2. Risk assessment by soil type

The risk of $N_2O$ emission was assessed according to the soil type. The results are shown in Figure 7.

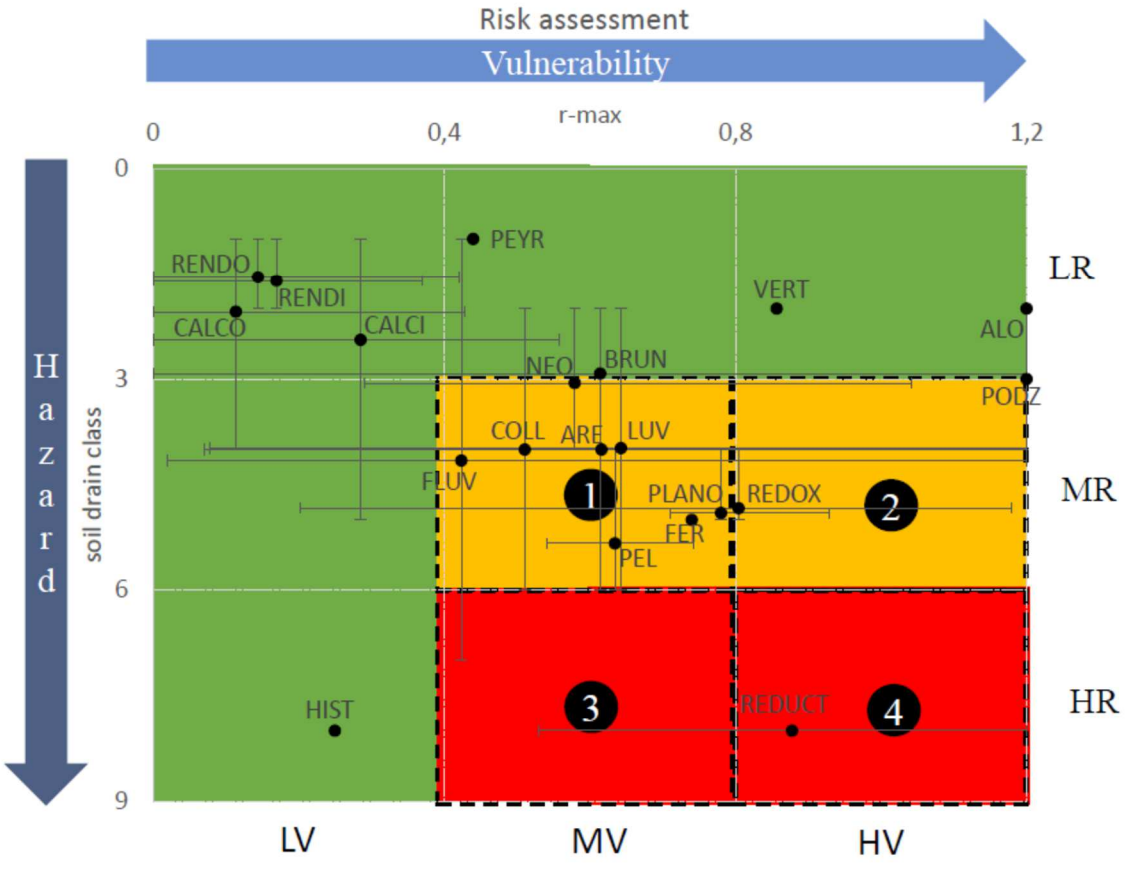


*Figure 7: risk by soil type based on their Vulnerability (mean r-max in x-axis) and Hazard ranges (mean drainage class in y-axis)). Bars indicate the min-max values of both r-max values and drainage*

*codes for each soil type. For clarity only the first letters of the name of soil types is given; see Table 2 and text for the full name.*

Only REDUCTISOLS are in risk situation "4" and some of the FLUVIOSOLS which may be in a significant situation of excess water are in risk situation "3". These two soil types are located in wetlands that are currently protected from excessive nitrogen inputs. They are mostly occupied by grasslands because the excess water does not allow cultivation.

Soils developped on limestone (CALCISOLS, CALCOSOLS, RENDISOLS and RENDOSOLS) do not present any risk of $N_2O$ emissions. HISTOSOLS, PEYROSOLS, VERTISOLS and ALOCRISOLS have no risk either, but there is only one value available to characterize them. PODZOSOLS have a High Vulnerability but the mean value of soil drain class is 3, thus the risk is between Low and Moderate. Podzosols are very poor and very acidic soils that are not conducive to agriculture.

All the others soils have a mid point in risk situation class "1" or "2". As soil types are generaly composed of several STU, some STU may be at risk of $N_2O$ emission and some others not, which is illustrated in the Figure 7 by bars crossing the dashed risk line. Some of BRUNISOLS, COLLUVIOSOLS, LUVISOLS, NEOLUVISOLS, PLANOSOLS and REDOXISOLS can be in moderate risk category (situations 1 or 2) depending on their *r-max* values and usually of acidity. High-risk situations of $N_2O$ emissions are not necessarily found in cultivated areas and are therefore not subject to high nitrogen Exposure. Indeed, very moist and acidic soils are not favourable to agriculture.

#### 3.2.3. Validation of the approach using a former dataset

399 Table 2 shows a very good consistency between $N_2O$ emission and Calc. *r-max* index. However, some
400 discrepancy exists between Calc. r-max index and STU r-max index (Table 2). This is owing to soil
401 map resolution. Nevertheless, all soil types are within the same risk class as shown in Figure 7.

*Table 2: Sites used for the validation and the measured properties during the field campaigns. The 3 first sites were taken from Hénault et al. (2005). SP sites were taken from Franqueville et al. (2018). ND4 is the same site as presented in Grossel et al. (2016) but flux data are unpublished. See these studies for more details. Note that SP5, SP6 and ND4 were sampled in both 2014 and 2015. SP7, SP8 and INRAE data are unpublished. Last column indicates the r-max index value calculated with the pedotransfer function of Hénault et al. (2019). Class risk estimated with the map soil typology.*

| | | Field measurements | | | | | | | | Donesol database | | | | | | |
|---|---|---|---|---|---|---|---|---|---|---|---|---|---|---|---|---|
| Site | Region | Period | $N_2O$ emission (g-N /ha) | N input (kg N/ha) | Measured r-max index | pH | CEC (cmol +.kg$^{-1}$) | Clay (g.kg$^{-1}$) | Calcultated r-max index | STU name | pH | CEC (cmol +.kg$^{-1}$) | Clay (g.kg$^{-1}$) | STU r-max index | Drain. class | classrisk |
| Villamblain (1999) | Beauce Dunoise | Feb - June 1999 | 517 | 230 | 0.2 | 7.9 | 22.8 | 334 | 0.23 | CALCISOLS | 8 | 20.8 | 341 | 0.13 | 2 | 0 |
| La Saussaye (1999) | Beauce | Feb - June 1999 | 376 | 164 | 0.2 | 7.8 | 16.5 | 242 | 0.2 | BRUNISOLS | 6.6 | 9.6 | 175 | 0.56 | 2 | 0 |
| Arrou (1999) | Faux-Perche | Feb - June 1999 | 2855 | 173 | 0.6 | 6.23 | 2.9 | 50 | 0.66 | LUVISOLS | 6.7 | 9 | 140 | 0.54 | 4 | 1 |
| SP1 (2014) | Faux-Perche | Feb - May 2014 | 696 | 142 | | 7.1 | 7.24 | 125 | 0.35 | LUVISOLS | 6.7 | 9 | 140 | 0.54 | 4 | 1 |
| SP3 (2014) | Faux-Perche | Feb - May 2014 | 950 | 140 | | 6.8 | 9.82 | 181 | 0.48 | COLLUVIOSOLS | 6.4 | 12.7 | 250 | 0.65 | 5 | 1 |
| SP5 (2014) | Faux-Perche | Feb - April 2014 | 986 | 170 | | 7 | 9.11 | 145 | 0.42 | LUVISOLS | 6.7 | 9 | 140 | 0.54 | 4 | 1 |
| SP6 (2014) | Faux-Perche | Feb - April 2014 | 2034 | 175 | | 6.3 | 8.06 | 237 | 0.58 | COLLUVIOSOLS | 6.3 | 8.1 | 230 | 0.59 | 5 | 1 |
| ND4 (2014) | Faux-Perche | Feb - April 2014 | 2781 | 175 | 0.66 | 6.3 | 6.81 | 141 | 0.65 | COLLUVIOSOLS | 6.4 | 12.7 | 250 | 0.65 | 5 | 1 |
| SP2 (2015) | Faux-Perche | Feb - May 2015 | 740 | 231 | | 6.4 | 6.82 | 140 | 0.61 | LUVISOLS | 6.7 | 9 | 140 | 0.54 | 4 | 1 |
| SP4 (2015) | Faux-Perche | Feb - May 2015 | 933 | 220 | | 6.5 | 9.82 | 137 | 0.65 | COLLUVIOSOLS | 6.4 | 12.7 | 250 | 0.65 | 5 | 1 |
| SP5 (2015) | Faux-Perche | Feb - May 2015 | 314 | 230 | | 7 | 9.11 | 145 | 0.42 | LUVISOLS | 6.7 | 9 | 140 | 0.54 | 4 | 1 |
| SP6 (2015) | Faux-Perche | Feb - May 2015 | 293 | 230 | | 6.3 | 8.06 | 237 | 0.58 | COLLUVIOSOLS | 6.3 | 8.1 | 230 | 0.59 | 5 | 1 |
| ND4 (2015) | Faux-Perche | Feb - May 2015 | 2118 | 230 | 0.66 | 6.3 | 6.81 | 141 | 0.65 | COLLUVIOSOLS | 6.4 | 12.7 | 250 | 0.65 | 5 | 1 |
| SP7 (2018) | Faux-Perche | Feb - May 2018 | 1550 | 240 | | 7.2 | 9.7 | 118 | 0.4 | LUVISOLS | 6.7 | 9 | 140 | 0.54 | 4 | 1 |
| SP8 (2018) | Faux-Perche | Feb - May 2018 | 1126 | 234 | | 6.6 | 8.8 | 118 | 0.58 | LUVISOLS | 6.7 | 9 | 140 | 0.54 | 4 | 1 |
| INRAE (2018) | Val de Loire | May - June 2018 | 200 | 100 | 0.61 | 6.23 | 2.9 | 50 | 0.66 | BRUNISOLS | 4.2 | 6.1 | 48 | 1.2 | 2 | 0 |

406

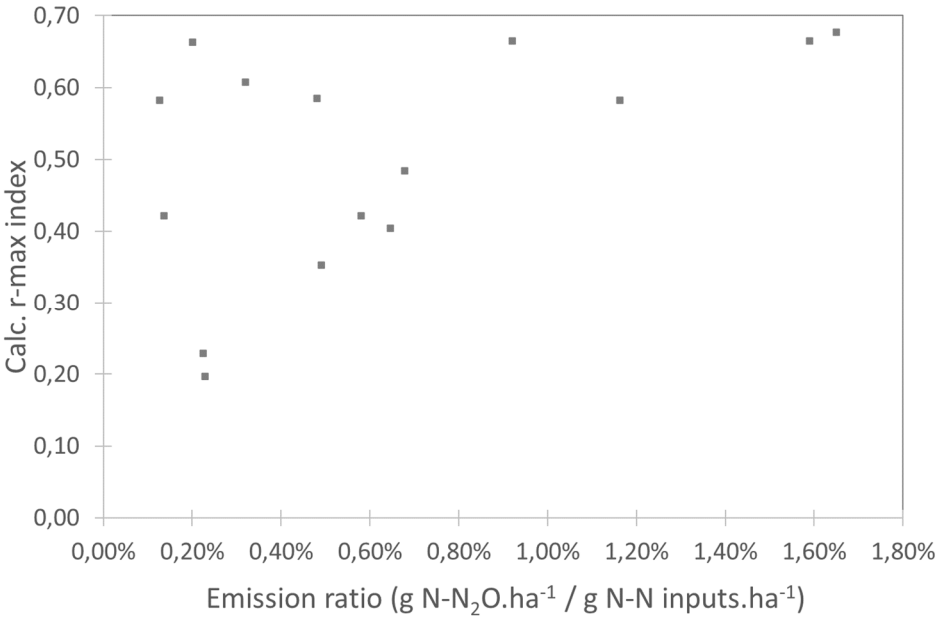


407

408 *Figure 9 : r-max index calculated based on measured soil properties versus emission ratio during*
409 *post-fertilization period.*

410 The risk class for each site was estimated (table 2). Only three sites were classified as risk class 0 (no
411 risk). One of them presented both low hazard and low vulnerability (Villamblain site) while the two
412 others presented medium vulnerability but low hazard (good drainage class) resulting in low emission
413 risk. For one of these sites, (La Saussaye) this was not consistent with direct observations because a
414 small r-max index was measured.

415 A risk class 1 was found for ten sites, corresponding to thirteen $N_2O$ emission values (three sites were
416 sampled in both 2024 and 2015). This could be explained by the fact that an area known for its
417 emissions is usually selected for such studies. There may therefore be a bias in favor of soils at risk
418 when choosing sites. However, no risk class greater than 1 was found.

419 To assess if soil classified as “at risk” indeed present largest $N_2O$ emission, Figure 10 shows the ratio
420 of cumulated $N_2O$ emission on N inputs during fertilization and post-fertilization period as a function
421 of class risk. During wet seasons, the ratio of $N_2O$ emission on N input was smaller on sites
422 presenting no risk (about 0.2%) than on sites presenting a risk class 1. Sites having a risk class 1

showed a large variability of the emission ratio, but it was always larger than 0.4%. In 2015, which was a rather dry year, only sites having a risk class 1 were studied. The emission ratio also presented a large variability but it was smaller than during wet seasons and some sites even presented emission ratio as low as the no risk sites during wet years. This is consistent with the hypothesis that risk is associated to hazard more than vulnerability because in dry conditions, even in hydromorphic soils, there is little denitrification.

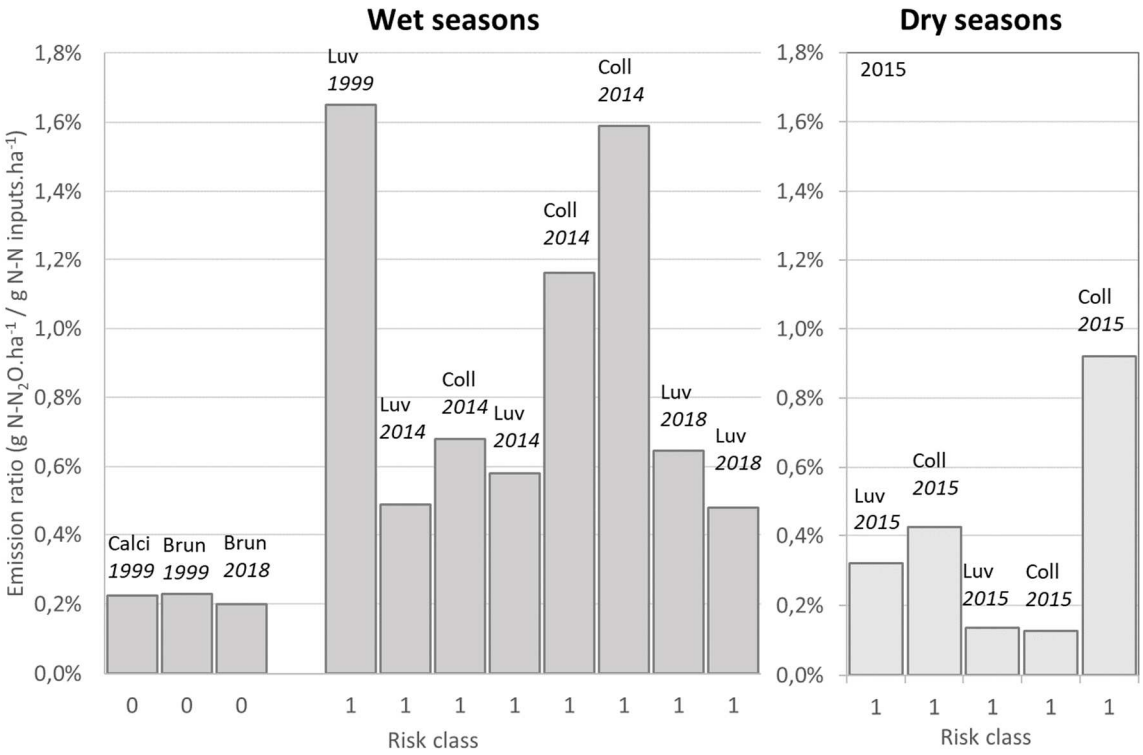


*Figure 10: $N_2O$ emission ratio versus soil risk class. Emission ratio is calculated as the ratio of cumulated emission of $N_2O$ during fertilization and post-fertilization period on N inputs and soil risk class is assessed through Donesol variables of the corresponding STU (see methodology part for more details). Left: observations made during wet climatic years, right: observations during normal to a dry climatic year. Emissions were cumulated over the fertilization periods, thus corresponding to different intervals (see Table 2).*

### 3.2.4.Risk mapping

Figure 8 (top) presents the percentage of area that present a risk of $N_2O$ emissions, and on the other maps (Figure 8, bottom), the risk is declined in the 4 situations described in Figure 4.

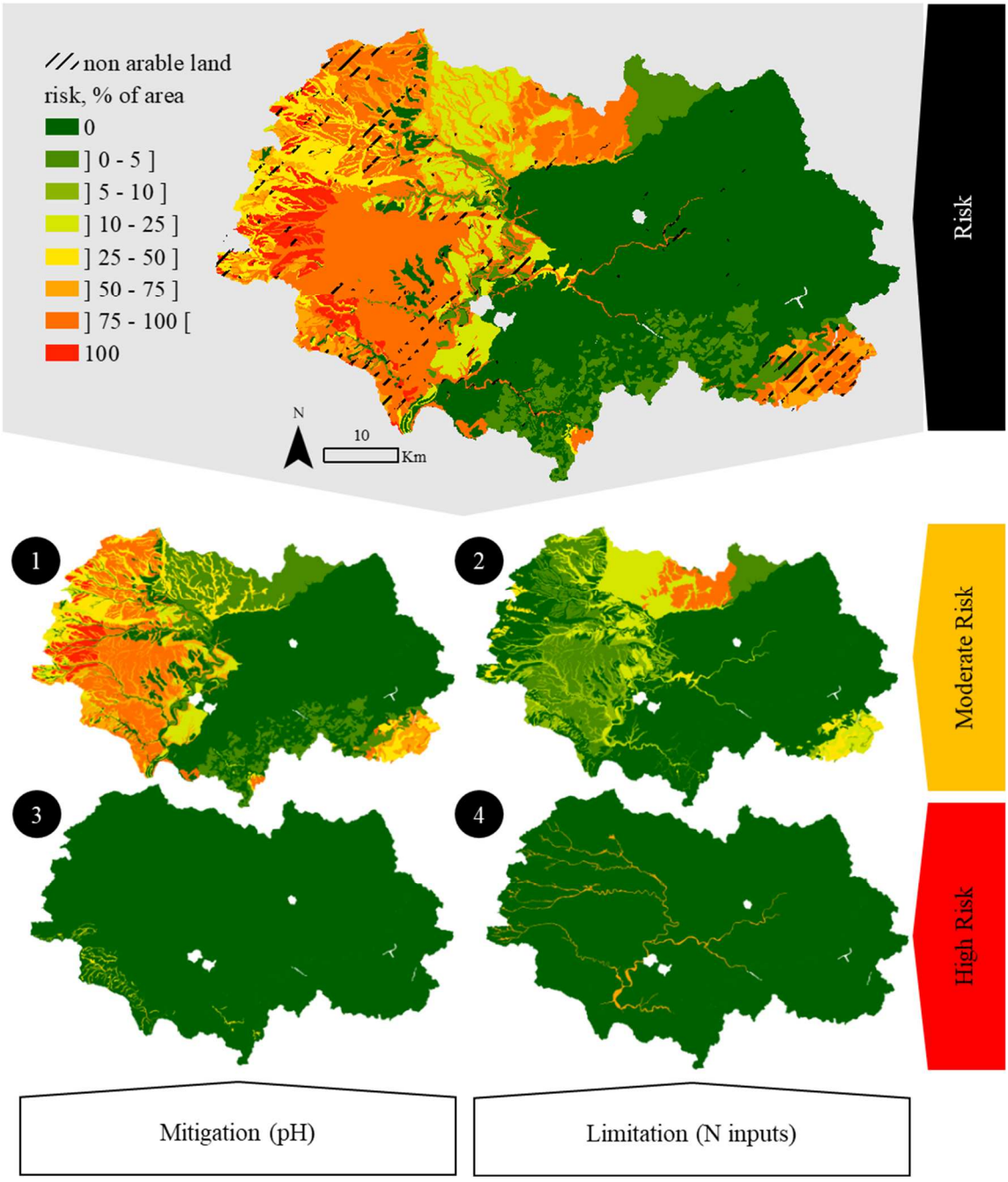


*Figure 8: Top. map of the relative area presenting $N_2O$ emission risk; bottom: maps of relative area of each emission risk categories 1, 2, 3 and 4. For risk category definition, see Figure 5.*

The risk situation is undefined for 15% of the total area. 53% of the surface present no risk of $N_2O$ emissions conversely to 32% of the total area. These 32 % can be split into 4 situations: 24 % in 1, 6%

445 in 2 , less than 1% in 3 and 1% in 4. Most of these risky soils are located in the Western Perche/Faux
446 Perche region, where 12% of the surface is covered by forest. Part of risky soils is also located in the
447 Orleans forest (Orléanais region), but these soils are not exposed to nitrogen inputs, risk does not exist
448 without exposure.

449 3.2.5. Uncertainties and strengths of the present approach

450 This approach of mapping emission risk can present several limitations. Firstly, as already written for
451 hazard and vulnerability maps, SMU aggregation entails uncertainties on the final risk map. To check
452 how reliable the two aggregation methods were, the risk for validation site was also estimated based
453 on SMU and not true STU (see supplementary material). Both SMU aggregation methods gave the
454 same risk class than the true STU corresponding to the sites. The methodology used for soil
455 classification also present uncertainties. The protocol for the *r-max* index measurements is based on
456 incubation with acetylene. The acetylene method can underestimate denitrification and ratio
457 $N_2O/(N_2O+N_2)$ because of several reasons, e.g. low diffusion of acetylene in intact soils and inhibition
458 of nitrification in field conditions (Groffman et al., 2006) so field assessment may be biased. The
459 present index is measured in artificial conditions: soil slurry amended with nitrate under agitation:
460 these conditions provide an index of the soil capacity of reduction to $N_2$ and not a direct measurement.
461 Reduction of $N_2O$ to $N_2$ can also be influenced in the fields by the soil nitrate and carbon availability
462 (Senbayram et al., 2012). However, the *r-max* index measured in the laboratory has been shown to
463 relate well with field $N_2O$ emissions (Hénault et al., 2005; Hénault et al., 2019). Last, only natural
464 drainage class from Donesol database was considered to define the hazard. Soil hydromorphy effect on
465 $N_2O$ emission can however be highly impacted by management practices: e.g. tile-drainage (Grossel et
466 al., 2016), tillage (Rochette et al., 2008), soil compaction (Pulido-Moncada et al., 2022).

467 The approach was evaluated by comparison with a limited database from in situ measurements and it
468 would be interesting to have further field data for validation. Moreover, field data also present
469 uncertainties : emissions were measured by manual static chambers and cumulative emissions has an
470 uncertainty linked to the frequency of measurements (Smith and Dobbie, 2001). Observed variability

is linked to the soil moisture dynamics, which is controlled not only by the precipitation regime but also the vegetation, tillage, and soil hydromorphy itself which can be due to the presence of a deep clay layer, position in topography (foot slopes) or contact with a water table. This can be illustrated by the site 5 (Franqueville et al., 2018) which was measured in 2014 and 2015. It was close to an intermittent river and soil hydromorphy is due to this vicinity (river water table). In spring 2015 the river dried out and $N_2O$ emissions ratio on N input was very low, while it was large in spring 2014. Last the variability of emissions is also controlled by the timing of fertilization and precipitations. The classification does not discriminate all field conditions but observations are consistent with the assessed soil classification for $N_2O$ emissions risk, suggesting that it can help distinguishing between risk level 0 and 1.

$N_2O$ emissions are controlled by a complex interplay of many factors, resulting in large variations both in time and space. N substrate is the main factor so many mitigation solutions have focused on applying N at optimal rate to limit surplus, using enhanced efficiency fertilizers, including nitrification inhibitors or introducing legumes in rotations (Luo et al., 2019; Kanter et al., 2020; Wagner Riddle et al., 2020). Although some solutions will benefit to any soil or climate type (such as health diet habit, Luo et al., 2019), identifying the riskiest areas for $N_2O$ emissions is also needed to target mitigation efforts (Cui et al., 2021). Site-specific management is proposed to mitigate local hotspots of $N_2O$ emissions but it has yet to be tested how this approach can apply at regional scale (Wagner-Riddle et al., 2020). This study proposes thus an approach to identify possible risk areas. This approach is based especially on a risk classification by soil types; soil type has indeed been long recognized as a control factor of $N_2O$ emission (Robertson 1989).

Identifying the risk factors could help proposing mitigation strategies. For 3/4 of the risky situations (risk classes 1 + 3), $N_2O$ emissions could be mitigated by regularly liming soil to maintain a pH around 6.8, as suggested by Hénault et al. (2019). Liming can have beneficial effects by reducing $N_2O$ emissions, while it can also increase agronomic risk (defficiency) and $CO_2$ emissions, but a recent meta-analysis suggested that, because of general yield increase, it may be beneficial (Zhang et al., 2022). Management based on liming should therefore still be assessed by local studies (Hénault et al.,

2019) and the present approach can also serve to guide where to conduct such studies. A third of other soils (risks 2 and 4), require a liming so-called "redress" action to avoid any risk. A soil drainage action does not prevent temporary water excess, but just limit this duration. It is best to avoid exposing soils to risk in too wet soil situations by not providing nitrogen. Farmers can predict these situations through the weather forecast or using soil moisture sensors. Theses situations are located at the edge of streams (The Loir and its tributaries), in areas with REDUCTISOLS and FLUVIOSOLS. It is not advisable to fertilize these soils areas, which are often classified as wetlands and which also cause problems with nitrate pollution.

The patterns of the risk map (Figure 8) are consistent with those of Lugato et al. (2017), who mapped mean $N_2O$ emission simulated on five years (supplementary material). Their map also showed two contrasting $N_2O$ emission areas with values from 1.09 kg N $ha^{-1}$ $yr^{-1}$ to 3.8 kg N $ha^{-1}$ $yr^{-1}$ for 2010 to 2014 at Haut-Loir. The added value of current paper is that it proposes maps of emission risk provided by soil types, rather than $N_2O$ emission, which are dependent on temporal variables such as precipitation regimes and agricultural practices. This enables also to propose action to be taken according to the risk situation. The *r-max* value (computed from soil clay content, CEC and pH) associated with a soil water excess indicator, available in French soil database, seems to be an efficient approach to define soil situations that require special care and help farmer to identify risky situation.

## Conclusion

A methodology to map $N_2O$ emission risk at regional scale based on soil properties was developed. Risk was defined by crossing a "vulnerability", defined by the low capacity of soil to reduce $N_2O$ in $N_2$ during denitrification, and "hazard", defined by the probability to have water excess and directly linked to soil drainage class. In the Haut-Loir watershed, 32% of soils presented $N_2O$ emission risks (when exposed to nitrogen fertilization), of which 75% could be mitigated by liming. Some soils (mainly the REDUCTISOLS in the valleys and some hydromorphic LUVISOLS), covering 7% of the watershed area, would require moreover special attention in nitrogen inputs. As the method is based

524 on knowledge of well-known factors controlling $N_2O$ production and reduction by denitrification and
525 as these data are accessible in soil databases, i.e. drainage class, pH, CEC and clay content, it could be
526 also applied to other regions. These risk maps can allow decision-makers to identify agricultural areas
527 that require special precautions to reduce agricultural $N_2O$ emissions.

528 Acknowledgements

529 We gratefully acknowledge N. Canal. This work was supported by the Region Centre, by the ADEME
530 (Agence de la Transition Ecologique, former Agence de l'Environnement et de la Maîtrise de
531 l'Energie, France) through the HydroGES project (grant 1660C0003) and by the Labex Voltaire
532 (ANR-10-LABX-100-01).

533 **Appendix A : soil correspondance RP 2008 to WRB 2006**

| *RP 2008* | *WRB 2006* |
|---|---|
| ALOCRISOLS | Cambisols Hyperdystric |
| ARENOSOLS | Arenosols |
| BRUNISOLS | Cambisols Eutric or Dystric |
| CALCISOLS | Cambisols Hypereutric |
| CALCOSOLS | Cambisols Calcaric |
| COLLUVIOSOLS | Colluvic Regosols |
| FERSIALSOLS | Haplic Luvisols |
| FLUVIOSOLS | Fluvisols |
| HISTOSOLS | Histosols |
| LUVISOLS | Haplic Luvisols or Haplic Albeluvisols or Luvisols |
| NEOLUVISOLS | Luvic Cambisols |
| PELOSOLS | Epistagnic regosols or Vertic Cambisols |
| PEYROSOLS | Hyperskelectic Leptosols or Hyperskelectic Podzols |
| PLANOSOLS | Planosols |
| PODZOSOLS | Podzols |
| REDOXISOLS | Stagnosols |
| REDUCTISOLS | Gleysols |
| RENDISOLS | Epileptic Cambisols Calcaric |
| RENDOSOLS | Epileptic Cambisols Hypereutric |
| VERTISOLS | Vertisols |

534

535

**References list:**


Baize, D. and Girard, M.C, 2009. Référentiel pédologique 2008. Versailles : Quae, 405 p. (Savoir Faire). ISBN 978-2-7592-0185-3. http://www.documentation.ird.fr/hor/fdi:010063397.

Billen, G., Ramarson, A., Thieu, V., Théry, S., Silvestre, M., Pasquier, C., Henault, C. and Garnier, J., 2018. Nitrate retention at the river–watershed interface: a new conceptual modeling approach. Biogeochemistry. 139, 31–51. https://doi.org/10.1007/s10533-018-0455-9.

Billen, G., Garnier, J., Grossel, A., Thieu, V., Théry, S., and Hénault, C., 2020. Modeling indirect $N_2O$ emissions along the N cascade from cropland soils to rivers. Biogeochemistry. 148, 207–221. https://doi.org/10.1007/s10533-020-00654-x.

Butterbach-Bahl, K., Baggs, E.M., Dannenmann, M., Kiese, R. and Zechmeister-Boltenstern, S., 2013. Nitrous oxide emissions from soils: how well do we understand the processes and their controls? Philos. Trans. R. Soc. Lond B Biol Sci. 368(1621): 20130122. https://doi: 10.1098/rstb.2013.0122.

Ciais, P., Sabine, C., Bala, G., Bopp, L., Brovkin, V., Canadell, J., Chhabra, A., DeFries, R., Galloway, J., Heimann, M., et al., 2013. Carbon and other biogeochemical cycles. Climate Change 2013: the physical science basis. Contribution of working group I to the fifth assessment report of the intergovernmental panel on climate change. Cambridge University Press Cambridge United Kingdom and New York NY USA , 465-570.

CITEPA, juillet 2021. Gaz à effet de serre et polluants atmosphériques. Bilan des émissions en France de 1990 à 2019. Rapport national d'inventaire/format SECTEN.

Crichton, D., 1999. The Risk Triangle. In: Ingleton, J., Ed., Natural Disaster Management, Tudor Rose, London, 102-103.

Cui, X., Zhou, F., Ciais, P., Davidson, E. A., Tubiello, F. N., Niu, X., ... & Zhu, D., 2021. Global mapping of crop-specific emission factors highlights hotspots of nitrous oxide mitigation. Nature Food, 2(11), 886-893.

Dobbie K.E. and Smith K.A. 2001. The effects of temperature, water-filled pore space and land use on $N_2O$ emissions from an imperfectly drained gleysol. Eur. J. Soil Sci. 52: 667–673

Franqueville, D., Benhamou, C., Pasquier, C., Hénault, C., & Drouet, J. L., 2018. Modelling reactive nitrogen fluxes and mitigation scenarios on a landscape in Central France. *Agriculture, Ecosystems & Environment*, *264*, 99-110

Groffman, P. M., Altabet, M. A., Böhlke, H., Butterbach-Bahl, K., David, M. B., Firestone, M. K., ... & Voytek, M. A., 2006. Methods for measuring denitrification: diverse approaches to a difficult problem. *Ecological applications*, *16*(6), 2091-2122.

Grossel, A., Nicoullaud, B., Bourennane, H., Lacoste, M., Guimbaud, C. Robert, C. and Hénault, C., 2016. The effect of tile-drainage on nitrous oxide emissions from soils and drainage streams in a cropped landscape in Central France. Agriculture. Ecosystems and Environment. 230, 251-260. https://doi.org/10.1016/j.agee.2016.06.015.

Gu, J., Nicoullaud, B., Rochette, P., Grossel, A., Hénault, C., Cellier, P. and Richard, G., 2013. A regional experiment suggests that soil texture is a major control of $N_2O$ emissions from tile-drained

winter wheat fields during the fertilization period. Soil Biology and Biochemistry. 60, 134-141. https://doi.org/10.1016/j.soilbio.2013.01.029.

Hénault, C., Devis, X., Page, S., Justes, E., Reau, R., Germon, J.C., 1998. Nitrous oxide emissions under different soil and land management conditions. Biol. Fertil. Soils. 26, 199-207.

Hénault, C., Bizouard, F., Laville, P., Gabrielle, B., Nicoullaud, B., Germon, J. C., and Cellier, P., 2005. Predicting in situ soil $N_2O$ emission using NOE algorithm and soil database. *Global Change Biology*, *11*(1), 115-127.

Hénault, C., Bourennane, H., Ayzac, A., Ratié, C., Saby, N.P.A. Cohan, J.-P., Eglin, T. and Le Gall, C., 2019. Management of soil pH promotes nitrous oxide reduction and thus mitigates soil emissions of this greenhouse gas. Sci Rep. 9(1):20182. https://doi.org/10.1038/s41598-019-56694-3.

Hergoualc'h, K., Akiyama, H., Bernoux, M., Chirinda, N., Del Prado, A., Kasimir, A., MacDonald, D., Ogle, S., Regina, K., van der Weerden, T., 2019. 2019 Refinement to the 2006 IPCC Guidelines for National Greenhouse Gas Inventories, Volume 5, Chapter 11: $N_2O$ emissions from managed soils, and $CO_2$ emissions from lime and urea application. Technical Report. Technical Report 4-88788-032-4, Intergovernmental Panel on Climate Change.

Hinton, N. J., Cloy, J. M., Bell, M. J., Chadwick, D. R., Topp, C. F. E., & Rees, R. M., 2015. Managing fertiliser nitrogen to reduce nitrous oxide emissions and emission intensities from a cultivated Cambisol in Scotland. Geoderma Regional, 4, 55-65.

Ito, A., Nishina, K., Ishijima, K., Hashimoto, S. and Inatomi, M., 2018. Emissions of nitrous oxide ($N_2O$) from soil surfaces and their historical changes in East Asia: a model-based assessment. Prog Earth Planet Sci. 5, 55. https://doi.org/10.1186/s40645-018-0215-4.

Kanter, D. R., Ogle, S. M., & Winiwarter, W., 2020. Building on Paris: integrating nitrous oxide mitigation into future climate policy. Current Opinion in Environmental Sustainability, *47*, 7-12.

Kasimir-Klemedtsson, Å., Klemedtsson, L., Berglund, K., Martikainen, P., Silvol, J. and Oenema, O., 1997. Greenhouse gas emissions from farmed organic soils: a review. Soil Use and Management. 13, 54, 245-250. https://doi.org/10.1111/j.1475-2743.1997.tb00595.x.

Kritee, K., Poville, J., Zavala-Araiza, D., Rudek, J., Ahuja, R. and Hamburg, S., 2018. Global risk assessment of high nitrous oxide emissions from rice production. A white paper by EDF partners. September 10, 2018. www.edf.org/sites/default/files/documents/EDF_White_Paper_Global_Risk_Analysis.pdf

Le Gall, C., Jeuffroy, M.-H., Hénault, C., Python, Y., Cohan, J.-P., Parnaudeau, V., Mary, B., Compère, P., Tristant, D., Duval, R. and Cellier, P., 2014. Analyser et estimer les émissions de $N_2O$ dans les systèmes de grandes cultures français. Innovations Agronomiques, INRA, 12, 97-112.

Lavell, A., Oppenheimer, M., Diop, C., Hess, J., Lempert, R., Li, J. et l., 2012. Climate Change: New Dimensions in Disaster Risk, Exposure, Vulnerability, and Resilience. In C. Field, V. Barros, T. Stocker, & Q. Dahe (Eds.), Managing the Risks of Extreme Events and Disasters to Advance Climate Change Adaptation: Special Report of the Intergovernmental Panel on Climate Change. Cambridge: Cambridge University Press. https://doi.org/10.1017/CBO9781139177245.004.

Lig'Air 2020, v2.4, mai 2020. Les émissions en région Centre-Val de Loire. Bilan de l'inventaire des émissions de polluants à effet sanitaire et gaz à effet de serre. Année de référence 2016 (et suivi temporel 2008 à 2016).

Lugato, E., Paniagua, L., Jones, A., de Vries, W., Leip, A., 2017. Complementing the topsoil information of the Land Use/Land Cover Area Frame Survey (LUCAS) with modelled $N_2O$ emissions. PLoS ONE. 12(4): e0176111. https://doi.org/10.1371/journal.pone.0176111.

Luo, Z., Lam, S. K., Fu, H., Hu, S., & Chen, D., 2019. Temporal and spatial evolution of nitrous oxide emissions in China: assessment, strategy and recommendation. Journal of cleaner production, *223*, 360-367.

Masson-Delmotte, V., Zhai, P., Pörtner, H. O., Roberts, D. C., Skea, J., Shukla, P. R., ... M Steg, L., 2018. Global warming of 1.5° C: Summary for policy makers.

Orsini, L. & Remy, J.C., 1976. Utilisation du chlorure de cobaltihexamine pour la détermination simultanée de la capacité d'échange et des bases échangeables des sols. Sci. Sol. Bull. de l'AFES, 4, 269-279.

Pulido-Moncada, M., Petersen, S. O., & Munkholm, L. J., 2022. Soil compaction raises nitrous oxide emissions in managed agroecosystems. A review. Agronomy for Sustainable Development, *42*(3), 38.

Richer-de-Forges, A.C., Arrouay, D., Bardy, M., Bispo, A., Lagacherie, P., Laroche, B., Lemercier, B., Sauter, J., Voltz, M., 2019. Mapping of Soils and Land-Related Environmental Attributes in France: Analysis of End-Users' Needs. Sustainability. 11(10), 2940. https://doi.org/10.3390/su11102940.

Rochette, P., Angers, D.A., Chantigny, M.H., Bertrand, N., 2008. $N_2O$ emissions respond differently to no-till in a loam and a heavy clay soil. Soil Sci. Soc. Am. J. 72, 5, 1363-1369. https://doi.org/10.2136/sssaj2007.0371.

Ruser, R., Schulz, R., 2015.The effect of nitrification inhibitors on the nitrous oxide ($N_2O$) release from agricultural soils-a review. J. Plant Nutrit. Soil Sci. 178 , pp. 171-188. https://doi.org/10.1002/jpln.201400251.

Russenes, A. L., Korsaeth, A., Bakken, L. R and Dörsch, P., 2016. Spatial variation in soil pH controls off-season $N_2O$ emission in an agricultural soil. Soil Biol Biochem. 99, 36–46. https://doi.org/10.1016/j.soilbio.2016.04.019

Senbayram, M., Chen, R., Budai, A., Bakken, L., and Dittert, K., 2012. $N_2O$ emission and the $N_2O/(N_2O+ N_2)$ product ratio of denitrification as controlled by available carbon substrates and nitrate concentrations. Agriculture, Ecosystems & Environment, 147, 4-12. https// doi:10.1016/j.agee.2011.06.022

Shaaban, M., Wu, Y., Wu, L., Hu, R., Younas, A., Nunez-Delgado, A., Xu, P., Sun, Z., Lin, S., Xu, X., Jiang, Y., 2020. The Effects of pH Change through Liming on Soil $N_2O$ Emissions. Processes. 8(6), 702. https://doi.org/10.3390/pr8060702.

Stehfest, E. and Bouwman, L., 2006. $N_2O$ and NO Emission from Agricultural Fields and Soils under Natural Vegetation: Summarizing Available Measurement Data and Modeling of Global Annual Emissions. Nutrient Cycling in Agroecosystems. 74, 207-228. https://doi.org/10.1007/s10705-006-9000-7.

Thompson, R.L., Lassaletta, L., Patra, P.K. et al., 2019. Acceleration of global $N_2O$ emissions seen from two decades of atmospheric inversion. Nat. Clim. Chang. 9, 993-998. https://doi.org/10.1038/s41558-019-0613-7.

Van Breemen, N. et Buurman, P., 2002. Hydromorphic Soils. Chapter 7, *Soil Formation*, p. 159-192. https://doi.org/10.1007/0-306-48163-4_7.

Wagner-Riddle, C., Baggs, E. M., Clough, T. J., Fuchs, K., & Petersen, S. O. (2020). Mitigation of nitrous oxide emissions in the context of nitrogen loss reduction from agroecosystems: managing hot spots and hot moments. Current Opinion in Environmental Sustainability, *47*, 46-53.

Wang, Y., Guo, J., Vogt, R. D., Mulder, J., Wang, J., & Zhang, X., 2018. Soil pH as the chief modifier for regional nitrous oxide emissions: new evidence and implications for global estimates and mitigation. Global Change Biology, 24(2), e617-e626.

WMO Greenhouse Gas Bulletin (GHG Bulletin), 2021- No. 17: The State of Greenhouse Gases in the Atmosphere Based on Global Observations through 2020.

Wolf, S., 2012. Vulnerability and risk: comparing assessment approaches. Nat Hazards. 61, 1099-1113. https://doi.org/10.1007/s11069-011-9968-4.

Zhang, H. M., Liang, Z., Li, Y., Chen, Z. X., Zhang, J. B., Cai, Z. C., ... & Abalos, D., 2022. Liming modifies greenhouse gas fluxes from soils: A meta-analysis of biological drivers. Agriculture, Ecosystems & Environment, *340*, 108182.